The Contribution of Acute Infarcts to Cerebral Small Vessel Disease Progression

Annemieke ter Telgte, MSc,[1]* Kim Wiegertjes, MSc,[1]* Benno Gesierich, PhD,[2] José P. Marques, PhD,[3] Mathias Huebner, PhD,[2] Jabke J. de Klerk, MSc,[1] Floris H. B. M. Schreuder, MD,[1] Miguel A. Araque Caballero, PhD,[2,4] Hugo J. Kuijf, PhD,[5] David G. Norris, PhD,[3] Catharina J. M. Klijn, MD,[1] Martin Dichgans, MD,[2,4,6] Anil M. Tuladhar, MD,[1] Marco Duering, MD,[2,6†] and Frank-Erik de Leeuw, MD[1†]

Objective: To determine the contribution of acute infarcts, evidenced by diffusion-weighted imaging positive (DWI+) lesions, to progression of white matter hyperintensities (WMH) and other cerebral small vessel disease (SVD) markers.
Methods: We performed monthly 3T magnetic resonance imaging (MRI) for 10 consecutive months in 54 elderly individuals with SVD. MRI included high-resolution multishell DWI, and 3-dimensional fluid-attenuated inversion recovery, T1, and susceptibility-weighted imaging. We determined DWI+ lesion evolution, WMH progression rate (ml/mo), and number of incident lacunes and microbleeds, and calculated for each marker the proportion of progression explained by DWI+ lesions.
Results: We identified 39 DWI+ lesions on 21 of 472 DWI scans in 9 of 54 subjects. Of the 36 DWI+ lesions with follow-up MRI, 2 evolved into WMH, 4 evolved into a lacune (3 with cavity <3mm), 3 evolved into a microbleed, and 27 were not detectable on follow-up. WMH volume increased at a median rate of 0.027 ml/mo (interquartile range = 0.005–0.073), but was not significantly higher in subjects with DWI+ lesions compared to those without ($p = 0.195$). Of the 2 DWI+ lesions evolving into WMH on follow-up, one explained 23% of the total WMH volume increase in one subject, whereas the WMH regressed in the other subject. DWI+ lesions preceded 4 of 5 incident lacunes and 3 of 10 incident microbleeds.
Interpretation: DWI+ lesions explain only a small proportion of the total WMH progression. Hence, WMH progression seems to be mostly driven by factors other than acute infarcts. DWI+ lesions explain the majority of incident lacunes and small cavities, and almost one-third of incident microbleeds, confirming that WMH, lacunes, and microbleeds, although heterogeneous on MRI, can have a common initial appearance on MRI.

ANN NEUROL 2019;86:582–592

Cerebral small vessel disease (SVD) constitutes the main vascular cause of cognitive impairment and dementia, and accounts for about one-fifth of all strokes.[1,2] SVD is further associated with gait impairment, mood disturbances, and late-life disability.[3] Conventional magnetic resonance imaging (MRI) markers of SVD include white matter hyperintensities (WMH), lacunes, and cerebral microbleeds, with WMH being the most widely studied.[2] Traditionally, WMH have been attributed to chronic cerebral hypoperfusion. However, evidence for this hypothesis remains inconclusive.[4,5]

View this article online at wileyonlinelibrary.com. DOI: 10.1002/ana.25556

Received Apr 17, 2019, and in revised form Jul 18, 2019. Accepted for publication Jul 18, 2019.

Address correspondence to Dr de Leeuw, Department of Neurology, HP 935, PO Box 9101, 6500 HB, Nijmegen, the Netherlands. E-mail: frankerik.deleeuw@radboudumc.nl

*A.t.T. and K.W. share first authorship.

†M.Du. and F.-E.d.L. share senior authorship.

From the [1]Department of Neurology, Donders Institute for Brain, Cognition and Behaviour, Radboud University Medical Center, Nijmegen, the Netherlands; [2]Institute for Stroke and Dementia Research (ISD), University Hospital, LMU Munich, Munich, Germany; [3]Donders Institute for Brain, Cognition and Behaviour, Centre for Cognitive Neuroimaging, Radboud University, Nijmegen, the Netherlands; [4]German Center for Neurodegenerative Diseases (DZNE Munich), Munich, Germany; [5]Image Sciences Institute, University Medical Center Utrecht, Utrecht, the Netherlands; and [6]Munich Cluster for Systems Neurology (SyNergy), Munich, Germany

Additional supporting information can be found in the online version of this article.

Correction added on 30th August, 2019, after first online publication: Affiliations 1–4 and 6 have been revised, and the running head has been updated throughout the article.

The limited understanding of the pathogenesis of SVD has several reasons. First, because SVD is rarely a cause of death, histopathology studies generally reflect advanced disease stages.[6] Moreover, such studies are by definition cross-sectional, limiting any causal inference. Finally, in vivo longitudinal studies are mostly conducted with follow-up intervals of several years,[5] impeding detailed mechanistic insights into SVD progression. Thus, novel in vivo study designs with highly frequent follow-ups are needed to gain further insight into SVD progression.

Only recently, a weekly MRI study applied over 16 weeks, among 5 individuals with SVD reported on an acute rather than chronic ischemic origin of WMH, as demonstrated by small acute diffusion-weighted imaging positive (DWI+) lesions that evolved into WMH on follow-up.[7] Because DWI+ lesions are frequently clinically silent, and only detectable within approximately the first 4 weeks,[8] they usually go unnoticed. It is estimated that the detection of a single DWI+ lesion at a random moment in time is indicative of hundreds of new cerebral microinfarcts per year.[9]

Recent studies show that DWI+ lesions may not only transform into WMH, but may also become a lacune or microbleed, or they may become invisible on follow-up scans.[2,10–13] Importantly, it is currently unknown what proportion of SVD progression can be explained by DWI+ lesions.

We hypothesized that DWI+ lesions drive progression of SVD markers, in particular WMH. Therefore, we conducted a prospective monthly MRI study, the RUN DMC – InTENse study (Radboud University Nijmegen Diffusion tensor and Magnetic resonance imaging Cohort–Investigating The origin and EvolutioN of cerebral small vessel disease),[14] and investigated the proportion of WMH progression explained by DWI+ lesions. In addition, we assessed the number of incident lacunes and incident microbleeds preceded by a DWI+ lesion.

Subjects and Methods

Study Design and Subjects

The prospective RUN DMC – InTENse cohort study was performed at the Radboud University Medical Center and the Donders Institute for Brain, Cognition, and Behaviour (Nijmegen, the Netherlands) between March 11, 2016 and November 3, 2017. Details of the study protocol have previously been published.[14] To summarize, this study comprised 12 visits to our research center, including a previsit, 10 consecutive monthly MRI visits, and a follow-up visit 1 year after the start of the study.

Subjects were selected from the previous prospective RUN DMC study, comprising MRI and clinical data collection in 2006, 2011, and 2015 among 503 patients with sporadic SVD referred to our Neurology Department.[15] Selection criteria for the RUN DMC – InTENse study were aimed at including 50 individuals with a high likelihood of progression of SVD imaging markers, while meticulously excluding those individuals with presumed causes of cerebral ischemia other than SVD. Therefore, inclusion criteria comprised participation in at least the RUN DMC 2006 and 2015 waves, WMH progression between 2006 and 2015 (those with largest WMH progression were invited first), and being able to visit our clinic monthly. The main exclusion criteria comprised a carotid artery stenosis >50% (either in the medical history or on ultrasound made during the previsit), a cardioembolic source (eg, atrial fibrillation; in the medical history or detected on electrocardiogram [ECG] during the previsit), use of oral anticoagulants, radiological or clinical evidence of a cortical ischemic stroke or transient ischemic attack, or vasculitis. Patients with any intracranial hemorrhage other than a microbleed on MRI or another pre-existing structural brain lesion preventing MRI analysis, dementia, Parkinson disease, 3T MRI contraindication, or a disease with life expectancy of <1 year were excluded. The RUN DMC – InTENse study was approved by the medical ethics committee region Arnhem–Nijmegen, and all subjects gave written informed consent prior to the start of the study.

MRI Acquisition

Subjects were scanned using a single 3T MRI scanner (MAGNETOM Prisma; Siemens Healthineers, Erlangen, Germany) and 32-channel head coil, including the following sequences (see also Supplementary Table 1 for further details):

- Multishell DWI, with 99 diffusion-weighted directions ($3 \times b = 200$, $6 \times b = 500$, $30 \times b = 1{,}000$, and $60 \times b = 3{,}000 s/mm^2$) covered uniformly within and across shells, $10 \times b = 0$ images (University of Minnesota, Center for Magnetic Resonance Research sequence), multiband acceleration factor = 3,[16] and 1.7mm isotropic voxels;
- One b = 0 image with opposite phase-encoding direction but acquisition parameters otherwise equal to the previous DWI sequence, to correct for susceptibility-induced distortions in DWI;
- Three-dimensional (3D) fluid-attenuated inversion recovery (FLAIR) with 0.85mm isotropic voxels;
- 3D T1-weighted using Magnetization Prepared 2 Rapid Acquisition Gradient Echoes (MP2RAGE) with 0.85mm isotropic voxels;
- 3D multiecho fast low-angle shot providing magnitude and phase images (6 echoes) to create susceptibility-weighted images with $0.8 \times 0.8 \times 2.0$mm voxels.

Automated checks of sequence parameters of all acquired images and standardized visual image quality control ensured high data quality.

Image Processing

Diffusion data were preprocessed for denoising and removal of Gibbs artifacts using tools from MRtrix (v3.0, http://www.

mrtrix.org).[17,18] Using eddy[19] and topup[20] within the Functional Magnetic Resonance Imaging of the Brain Software Library (FSL; v5.0), raw diffusion data were corrected for susceptibility-induced distortions, motion, and eddy currents. Intensity bias correction was performed with N4 bias correction as implemented in Advanced Normalization Tools, version 2.1.0.[21] Diffusion-weighted trace images were generated for the b = 1,000 and b = 3,000 images based on the arithmetic mean across diffusion directions. Using dtifit in FSL, we calculated the mean diffusivity map utilizing the b = 1,000 shell. The mean diffusivity map is equivalent to the apparent diffusion coefficient, but derived from a diffusion tensor model.[22]

FLAIR images were bias corrected using the N4 bias correction procedure.

MP2RAGE data were processed to obtain robust T1-weighted images, which constitute the best compromise between image intensity bias and increased noise levels in the image background and cavities of the skull. This was done according to a previously described procedure,[23] using custom-written scripts in MATLAB (R2016b; MathWorks, Natick, MA).

To generate susceptibility-weighted images, for each of the 6 echo times we multiplied high-pass filtered (filter size = 12 pixels) phase images with their corresponding magnitude images, which were subsequently averaged into a single susceptibility-weighted imaging (SWI) scan.

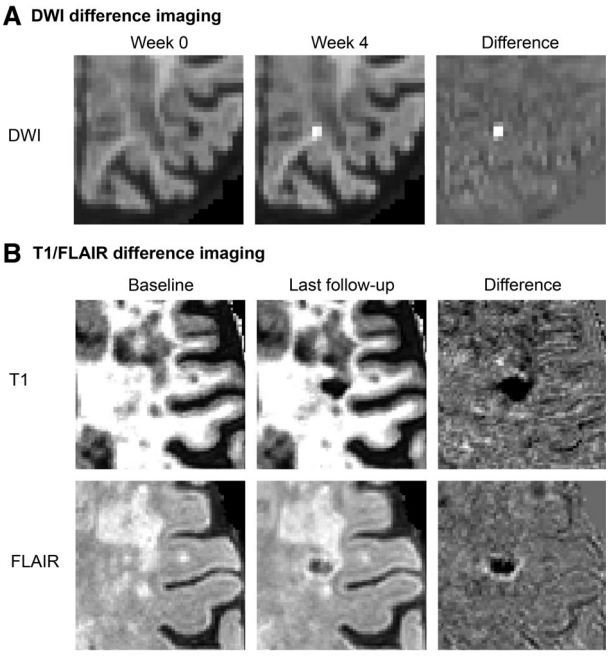

FIGURE 1: Incident lesion detection using difference imaging. (A) Diffusion-weighted imaging (DWI) difference images were created by subtracting registered DWI trace images (shown here b = 3,000) from consecutive magnetic resonance imaging (MRI) visits to detect incident DWI+ lesions. (B) Incident lacunes were detected on T1 and fluid-attenuated inversion recovery (FLAIR) difference images created by subtracting registered baseline T1 and FLAIR scans from the last available follow-up scan.

To facilitate the systematic detection of incident lesions, difference images were generated for the DWI (both b = 1,000 and b = 3,000 trace images), FLAIR, and T1 image modalities. For this purpose, we first skull stripped the images using the Brain Extraction Tool in FSL and normalized the image intensity to the 95th percentile. Next, we registered (within each modality) the images of all different MRI visits to a subject-specific template, generated using FreeSurfer's mri_robust_template.[24] Difference images were then created by subtracting registered and intensity-normalized images from consecutive MRI visits, thereby highlighting incident SVD lesions as an easily discoverable hyperintense or hypointense voxel cluster on a uniform background (Fig 1).[25]

Assessment of MRI Markers of SVD and Lesion Evolution

SVD lesions were assessed blinded to clinical characteristics according to the previously published STandards for ReportIng Vascular changes on nEuroimaging (STRIVE).

To detect DWI+ lesions, one rater (A.t.T.) manually screened all available difference images. The mean diffusivity map was assessed to verify a hypointense or isointense signal at the corresponding lesion location. A second rater (K.W.) screened all positive scans, together with a random set of 50 negative scans (~10%). Cohen's kappa was 0.78 (95% confidence interval [CI] = 0.62–0.95), and Dice similarity coefficient (DSC) was 0.86, indicating good inter-rater agreement. After final consensus was reached, both raters manually segmented all DWI+ lesions on the b = 3,000 native trace image to calculate lesion volume. Median DSC on the entire set of DWI+ lesions was 1.0 (interquartile range [IQR] = 0.8–1.0), indicating high spatial overlap between the segmentations of the two raters.

WMH were segmented using an automatic algorithm based on deep fully convolutional network and ensemble models.[26] Input images were the native space FLAIR images together with the registered T1-weighted images. This algorithm was chosen because it was ranked first in the WMH Segmentation Challenge at MICCAI 2017. WMH volumes were extracted from the resulting binary WMH masks. To address variability present in the WMH segmentation results, we calculated predicted individual WMH volume (at each time point) and rate of WMH change (ml/mo), using all time points and a simple linear regression model on WMH volumes over time (Fig 2), and report here the WMH volumes as volumes predicted by this linear model. To account for atrophy, WMH volumes were also expressed as percentage of total white matter volume, estimated at each time point from robust T1-weighted images using the Statistical Parametric Mapping (SPM) toolbox tissue segmentation algorithm (v12; Wellcome Department of Cognitive Neurology, London, UK; http://www.fil.ion.ucl.ac.uk/spm). Given that WMH are often misclassified by SPM as cerebrospinal fluid or gray matter, the white matter mask was corrected using the WMH mask.

To detect lacunes, we followed a consensus rating strategy, as inter-rater agreement of lacune detection is known to be low.[27] Two raters (A.t.T., J.J.d.K.) performed a sensitive rating of all baseline FLAIR and T1-weighted images to identify possible baseline

lacunes, and subsequently, all difference FLAIR and T1-weighted images representing the change from baseline to last available follow-up to identify possible incident lacunes. Final decisions were made in consensus involving more raters (M.Du., F.-E.d.L.).

To detect microbleeds, one rater (K.W.) visually screened possible microbleeds (including lesions with axial diameter < 2mm) detected by a semiautomatic method based on the radial symmetry transform, including minimum intensity projection, which improves sensitivity and reduces the number of possible locations.[28] True microbleeds were selected by the human rater. A second rater (J.J.d.K.) screened all positive cases plus a random set of 25 negative cases (~5%). Cohen's kappa was 0.70 (95% CI = 0.46–0.86) and the DSC was 0.67, indicating good inter-rater agreement. Final consensus was reached involving a third rater (F.H.B.M.S.).

The evolution of DWI+ lesions was determined by consensus (A.t.T., K.W., M.Du., F.-E.d.L.) using the last available FLAIR, T1-weighted, and SWI scans, and included the following categories: WMH, lacune or small incident cavity (to include incident cavities with axial diameter <3mm, which are currently not covered by STRIVE), microbleed, and disappearance or almost vanished (ie, very subtle tissue alteration, which can only be seen with prior knowledge of the DWI+ lesion). To assess lesion evolution, images of the different modalities (DWI, FLAIR, and SWI) were affine registered to the T1-weighted image of the same visit. Next, T1-weighted images of the monthly follow-up visits were affine registered to the T1-weighted image of the first MRI visit. The estimated transformations were applied to the coregistered images of the other modalities and lesion masks. All transformations were done using Advanced Normalization Tools (v2.1.0).[29]

Clinical Characteristics

Cardiovascular risk factors were assessed during the previsit (unless otherwise specified) and defined as follows: hypertension as a mean systolic blood pressure ≥140mmHg and/or diastolic blood pressure ≥90mmHg and/or use of an antihypertensive drug; diabetes as a random glucose ≥11.1mmol/l, or an overnight fasting glucose ≥7.0mmol/l measured at least 1 month later, and/or use of an antidiabetic drug; hypercholesterolemia as fasting total cholesterol levels ≥6.5mmol/l measured in parallel with the third MRI scan, and/or use of a lipid-lowering drug; smoking status as ever or never smoked; body mass index as weight over height squared. In addition, we assessed use of antithrombotic agents, educational level using a 7-point Dutch rating scale, and the Mini-Mental State Examination score during the previsit.

Statistical Analysis

All statistical analyses were performed in R (v3.4.3–4; https://www.R-project.org). We determined the cumulative incidence of DWI+ lesions, as well as their median monthly incidence on the basis of the DWI+ lesion incidence per MRI visit. Demographic, clinical, and baseline MRI characteristics were compared between subjects with versus without any DWI+ lesion during the study period, using nonparametric tests. WMH progression rate, and incidence of lacunes (and small cavities) and microbleeds were also compared between these groups. We determined the proportion of the total WMH progression that could be attributed to a DWI+ lesion per individual as follows: DWI lesion volume/total predicted WMH volume increase. The 2-tailed significance level α was set at 0.05. To take into account that we could have missed a DWI+ lesion due to missing data, individuals with an incident lesion without DWI 1 month prior to the event were excluded from the analysis where appropriate.

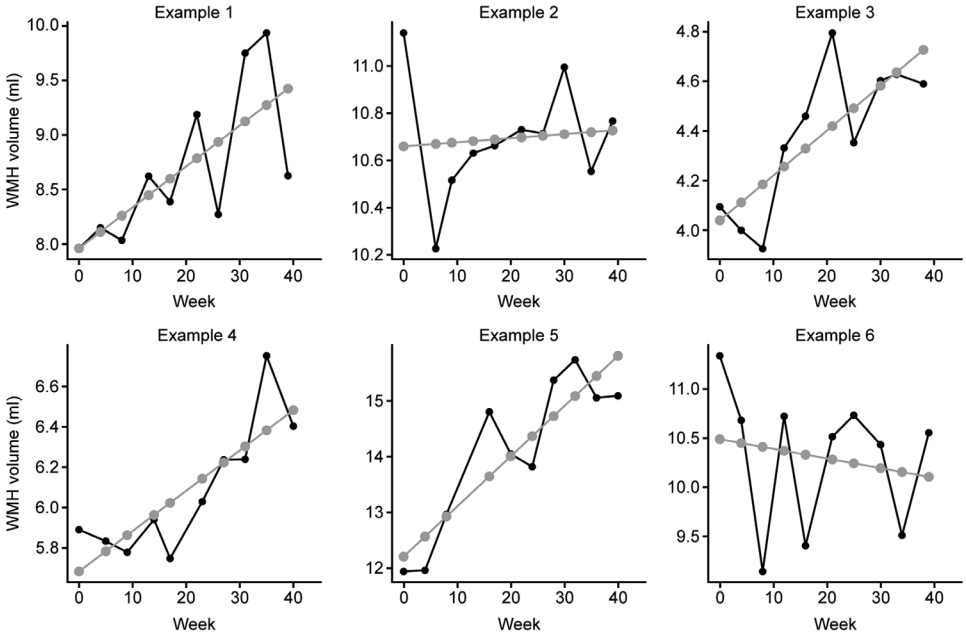

FIGURE 2: Predicted change of white matter hyperintensity (WMH) volume. On the basis of WMH volumes measured at each time point (black) and a simple linear regression model on WMH volumes over time (gray), rate of WMH change was calculated per subject (ie, the slope of the regression model). To address variability present in the WMH segmentation results, we reported the WMH baseline volumes as volumes predicted by this linear model.

Results

Characteristics of Cohort

The RUN DMC – InTENse cohort comprised 54 subjects with sporadic SVD (Fig 3). Median baseline age was 69 years (IQR = 66–74) and 63% was male. Of the 54 subjects, 39 had 10 complete MRI datasets, whereas 2 subjects never had follow-up MRI (see Fig 3B). In total, 472 DWI scans were collected. The median duration of follow-up was 39.5 weeks (IQR = 37.8–40.3), with a median MRI interval of 31.2 days (IQR = 30.0–32.3).

Incidence of DWI+ Lesions

In total, 39 DWI+ lesions were observed in 9 of 54 (16.7%) subjects (21/472 scans), resulting in a median monthly incidence of DWI+ lesions of 4.4% (95% CI = 3.9–5.8). Four subjects had a single DWI+ lesion. Two subjects had 2 DWI+ lesions on a single MRI, and 3 subjects had multiple DWI+ lesions (n = 7, 8, and 16) on multiple MRI scans (n = 6, 6, and 3, respectively). The median volume of DWI+ lesions was 0.010ml (IQR = 0.010–0.032). All DWI+ lesions were silent in the sense that none of the subjects experienced a clinical event in the respective interval between visits.

DWI+ lesions were distributed throughout the brain, with 32 (82%) being supratentorial (Fig 4; Supplementary Video 1). These were located in the white matter (n = 5), subcortical gray matter (n = 3), cortex (n = 22), and the cortical gray–white matter junction (n = 2). All 7 (18%) infratentorial DWI+ lesions were located in the cerebellar cortex.

Compared to subjects without DWI+ lesions, subjects with a DWI+ lesion were older (p = 0.004). Median WMH volume was >2-fold higher in subjects with DWI+ lesions compared to those without (9.0 vs 3.8ml), although this difference did not reach statistical significance (p = 0.214), possibly due to the small sample size. Similarly, no other statistical differences with respect to demographic, clinical, and MRI characteristics were observed between the two groups (Table 1).

Evolution of DWI+ Lesions

Follow-up scans were available for 36 (92%) DWI+ lesions. Two DWI+ lesions evolved into a WMH, one into a lacune ≥3mm and 3 into a small cavity <3mm. Three DWI+ lesions evolved into a microbleed, with 2 lesions further being hyperintense on T2 in the acute phase and on follow-up. Twenty-five DWI+ lesions disappeared or almost vanished on follow-up FLAIR and T1, despite having shown a FLAIR and/or T1 signal change in the acute phase. The majority of lesions that disappeared were located in the cortex. Two DWI+ lesions never became visible on FLAIR and T1, either in the acute phase or on follow-up (Table 2; Fig 5; Supplementary Video 2).

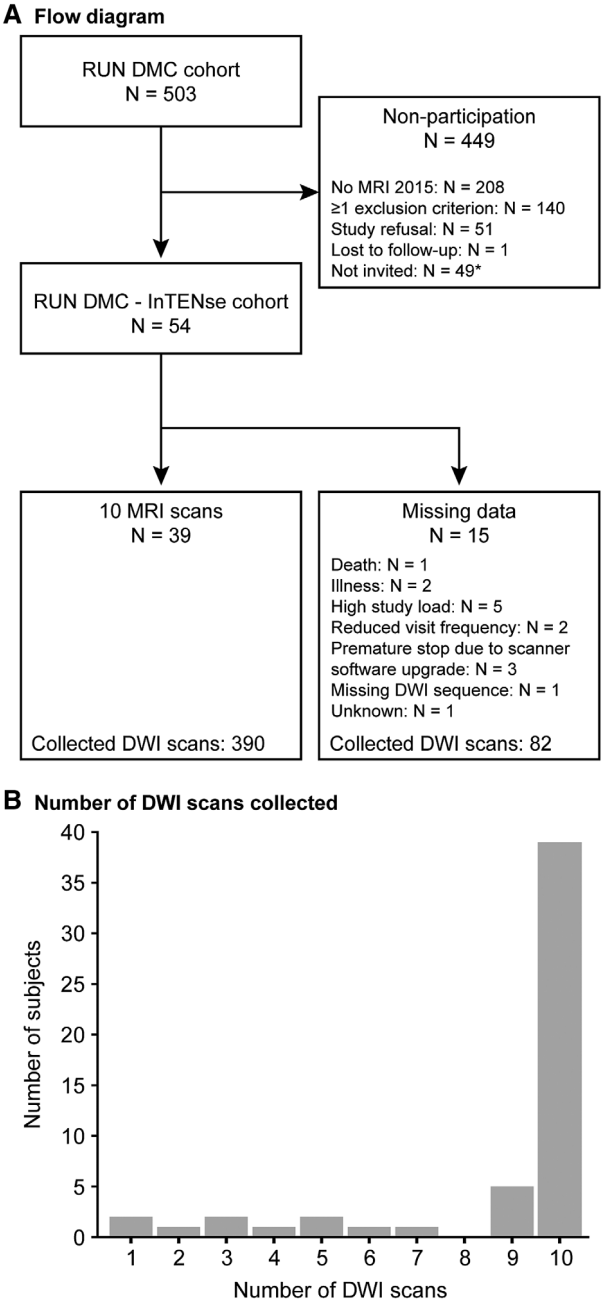

FIGURE 3: Flow diagram of the RUN DMC – InTENse cohort and number of diffusion-weighted imaging (DWI) scans collected. *Forty-nine subjects from the RUN DMC cohort were not invited because the intended sample size had been achieved. MRI = magnetic resonance imaging.

Contribution of DWI+ Lesions to Total SVD Progression

The volume of WMH increased at a median rate of 0.027 ml/mo (IQR = 0.005–0.073). However, WMH progression rate was not higher in subjects with ≥1 incident DWI+ lesions compared to those without (p = 0.195;

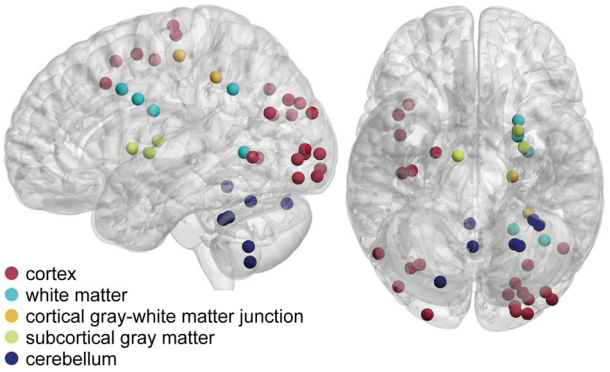

FIGURE 4: Distribution of diffusion-weighted imaging positive (DWI+) lesions. The distribution of DWI+ lesions is depicted in Montreal Neurological Institute–152 standard space. The image was created using BrainNet Viewer (http://www.nitrc.org/projects/bnv/).

Table 3), also after correction for white matter atrophy (p = 0.282, data not shown). Of the 2 cases with evolution of a DWI+ lesion into a WMH, the DWI+ lesion contributed to 23% of the total increase in the WMH in one case, whereas in the other case there was a regression of WMH volume.

Analyzing FLAIR and T1 difference images, we found 6 incident lacunes or small incident cavities in 3 of 52 (5.8%) subjects over the entire study period. One subject had an incident lacune without DWI 1 month prior to the event, and was therefore excluded from the subsequent statistical analysis. The incidence of lacunes and small incident cavities was significantly higher in subjects with a DWI+ lesion (p = 0.028; see Table 3) compared to those without. DWI+ lesions preceded 4 of 5 (80%) incident lacunes or small incident cavities at the corresponding location.

Analyzing the SWI scans, we found 10 incident microbleeds in 6 of 52 (12%) subjects over the entire study period. These incident microbleeds occurred in 3 of 9 subjects with a DWI+ lesion, and 3 of 43 without DWI+ lesions (p = 0.057; see Table 3). DWI+ lesions preceded 3 of

TABLE 1. Baseline Characteristics

Characteristic	No DWI+ Lesion, n = 45	DWI+ Lesion, n = 9	p
Demographic			
Age, yr	68 (65–72)	76 (69–82)	0.004[a]
Men	27 (60%)	7 (78%)	0.458
Level of education	5 (5–6)	5 (5–6)	0.883
Clinical			
MMSE	29 (28–30)	28 (28–30)	0.363
Antithrombotic agents	21 (47%)	5 (56%)	0.724
Hypertension	37 (82%)	8 (89%)	1.000
Diabetes	3 (7%)	3 (33%)	0.051
Hypercholesterolemia	22 (49%)	5 (56%)	1.000
BMI, kg/m^2	25 (24–28)	26 (25–28)	0.634
Smoking, ever	32 (71%)	6 (67%)	1.000
MRI			
WMH volume, ml	3.8 (2.2–10.2)	9.0 (5.1–10.5)	0.214
WMH volume, % of WM volume	1.0 (0.5–2.3)	2.1 (1.5–3.2)	0.181
Lacunes, prevalence	9 (20%)	3 (33%)	0.399
Microbleeds, prevalence	19 (42%)	6 (67%)	0.275
WM volume, ml	426 (395–462)	400 (379–446)	0.493

Data are median (interquartile range) or number (%). Level of education was determined using a 7-point Dutch rating scale ranging from primary school not completed (1) to academic degree (7).

[a]Statistically significant.

BMI = body mass index; DWI+ = diffusion-weighted imaging positive; MMSE = Mini-Mental State Examination; MRI = magnetic resonance imaging; WM = white matter; WMH = white matter hyperintensity.

TABLE 2. Evolution of DWI+ Lesions according to Lesion Location

	Evolution						
Location of DWI+ lesion	WMH	Lacune/Small Incident Cavity	Microbleed	Microbleed with T2 Hyperintensity	Disappearance/ Almost Vanished	Other	Follow-up Not Available
Cerebrum							
White matter	1	3	0	0	0	0	1
Subcortical gray matter	0	1	0	1	1	0	0
Cortex	0	0	0	0	20	1[a]	1
Cortical gray–white matter junction	1	0	0	0	0	1[a]	0
Cerebellum							
Cortex	0	0	1	1	4	0	1

The evolution of DWI+ lesions was determined using the last available FLAIR, T1-weighted, and susceptibility-weighted imaging scans. Shown are the locations of the DWI+ lesions in rows and the evolution in columns.
[a]Both lesions were never visible on FLAIR and T1-weighted imaging.
DWI+ = diffusion-weighted imaging positive; FLAIR = fluid-attenuated inversion recovery; WMH = white matter hyperintensity.

10 (30%) incident microbleeds at the corresponding location.

Discussion

In this monthly MRI study of individuals with sporadic SVD, we found clinically silent DWI+ lesions in almost one-fifth of subjects, resulting in a monthly incidence of 4.4%. However, DWI+ lesions explained only a small proportion of the total WMH volume increase. In addition to WMH, DWI+ lesions preceded 80% of incident lacunes or small cavities, and 30% of incident microbleeds. Cortical DWI+ lesions mostly disappeared on follow-up MRI.

The observed incidence of DWI+ lesions is in line with previous cross-sectional studies.[9] However, the cumulative incidence of DWI+ lesions of 17% during the course of our study is much lower compared to a small longitudinal case series in which 3 of 5 (60%) individuals with SVD developed DWI+ lesions within the white matter during a 16-week period.[7] This discrepancy is most likely related to the difference in SVD burden. Whereas all cases from the previous case series had moderate to severe SVD (Fazekas ≥2), our study included participants with an on average lower but wider range of SVD burden, with approximately 50% of the cohort having a Fazekas score ≥ 2.

In the present study, we demonstrated a differential evolution of DWI+ lesions, corroborating recent findings.[2,10–13] Although factors determining lesion evolution remain largely unclear, our data show that markers of SVD that are heterogeneous on MRI can have a common initial appearance on MRI.

The contribution of DWI+ lesions to WMH progression was, however, minor. Thus, we could not confirm the hypothesis that DWI+ lesions are the major cause of WMH. Two factors could potentially have led to an underestimation of the role of DWI+ lesions in WMH progression. First, despite the rather high resolution and high quality of the DWI scans, small DWI+ lesions, below the 1.7mm voxel size, might have gone undetected, and consequently their conversion into incident WMH might have been missed, because the DWI resolution was lower than the FLAIR resolution.[9,30] Second, as a result of our monthly MRI frequency, DWI+ lesions could have gone unnoticed for which the DWI signal was increased only shortly. It seems, however, more likely that WMH are mostly driven by factors other than acute ischemia, including blood–brain barrier disruption, demyelination, and inflammation.[4,6,31] Future work is required to unravel how these different pathological mechanisms are related in time. In contrast, we revealed that DWI+ lesions are the major cause of incident lacunes and small incident cavities.

This study highlights 2 further interesting findings, which require future investigations. First, in contrast to most previous studies, many DWI+ lesions were located in the cortex, with the majority of these lesions meeting the size criteria of acute cortical microinfarcts (<5mm).[9] Previous studies may simply have been unable to detect these microinfarcts due to limited resolution of the DWI scans.

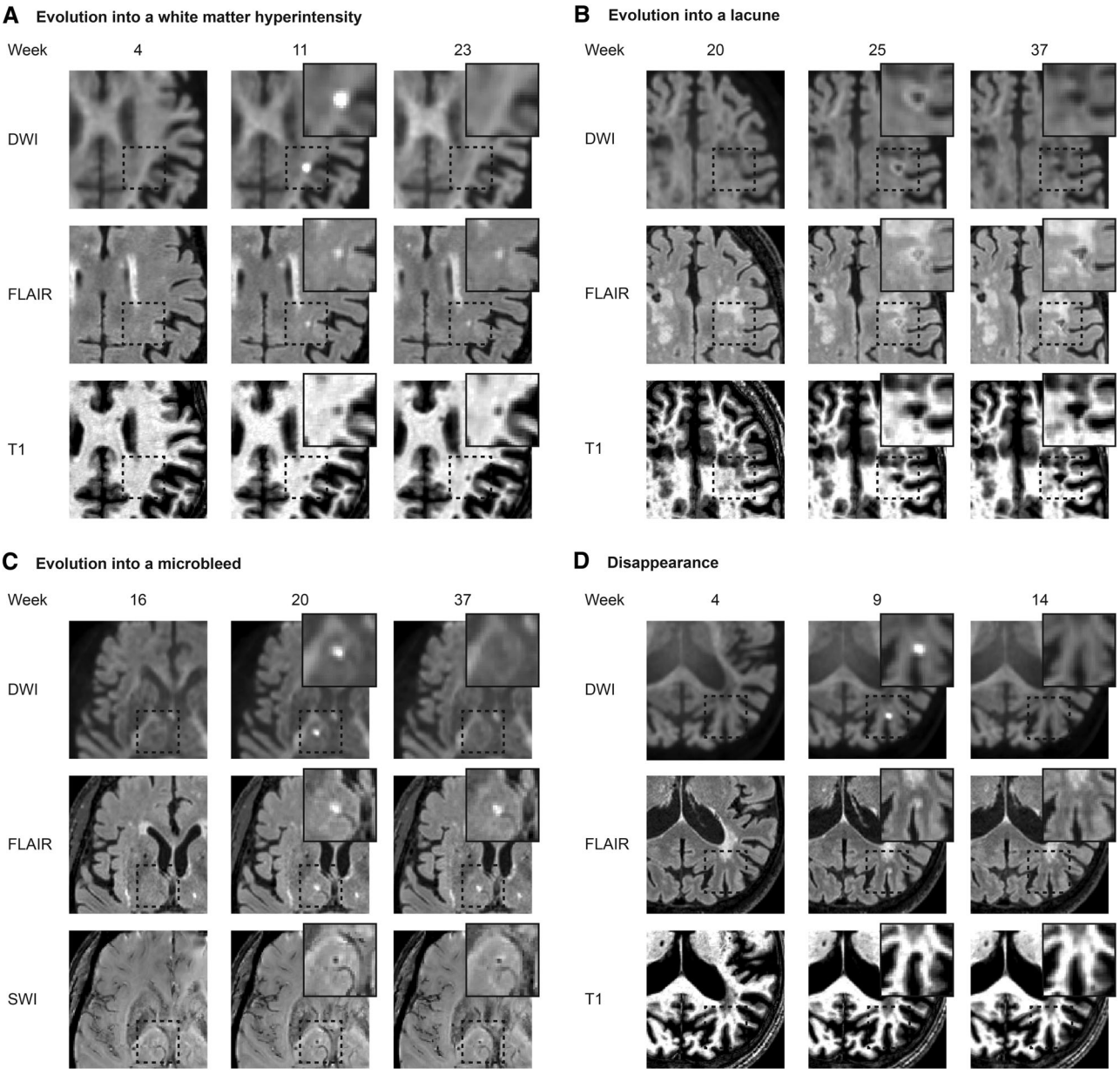

FIGURE 5: Differential evolution of diffusion-weighted imaging positive (DWI+) lesions. Each panel shows b = 3,000 DWI trace images. Prelesional scans (left) and last available follow-up scans (right) are shown. FLAIR = fluid-attenuated inversion recovery; SWI = susceptibility-weighted imaging.

Second, the vast majority of cortical lesions disappeared on follow-up MRI. In line with our findings, one recent study among patients with transient ischemic attack demonstrated DWI+ lesion disappearance, with cortical topography and small lesion size being important predictors for lesion disappearance.[32] Based on animal studies, we hypothesize, however, that lesion disappearance does not imply full recovery.[33] More likely, these small acute infarcts cause microscopic tissue injury below the T1 and FLAIR detection limit. Nonetheless, when accumulating over time, these microscopic lesions may contribute to cortical atrophy and cognitive decline.[34]

SVD is now recognized as the most important vascular contributor to dementia, but a causal treatment directed at preventing the development or slowing the progression of SVD does not yet exist. Our findings indicate DWI+ lesions as a marker of SVD, and therapeutic strategies aimed at the prevention of acute ischemic DWI+ lesions could contribute to halting part of the progression of SVD. Among patients with vascular cognitive impairment, the presence of acute microinfarcts was associated with a 2-year poor clinical outcome, suggesting their value as an imaging target in future trials.[35] However, due to the limited detection window of DWI+ lesions, high-frequent

TABLE 3. Progression of SVD MRI Markers and Proportion Explained by DWI+ Lesions

	No DWI+ Lesion, n = 43	DWI+ Lesion, n = 9	*p*	Incident MRI Markers of SVD Preceded by a DWI+ Lesion
WMH progression, ml/mo	0.033 (0.008–0.067)	−0.001 (−0.039 to 0.137)	0.195	
Lacunes, incidence	0 (0%)	2 (22%)	0.028[a,b]	4/5 (80%)
Microbleeds, incidence	3 (7%)	3 (33%)	0.057	3/10 (30%)

Data are median (interquartile range) or number of subjects with an incident lesion (%).
[a]Statistically significant.
[b]One subject with an incident lacune but without DWI one month prior to the event was excluded from this analysis.
DWI+ = diffusion-weighted imaging positive; MRI = magnetic resonance imaging; SVD = small vessel disease; WMH = white matter hyperintensity.

imaging is required, which might be a critical limitation for clinical trials.

The prospective study design and the acquisition of 10 monthly serial MRIs make this study powerful and unique. A major strength of the study is the high quality of the MRI protocol. We acquired high-resolution isotropic multishell DWI, including a b = 3,000 shell, which is superior to b = 1,000 for the detection of small hyperacute DWI+ lesions,[36] in combination with high-resolution 3D FLAIR, 3D T1, and 3D SWI scans. As a result, we were able to detect incident lesions with axial dimensions below the defined STRIVE criteria,[6,9] and characterize DWI+ lesion evolution in more detail, including small cavities without fluid suppression on FLAIR and hemorrhagic transformation. The 3 small incident cavities and 2 microbleeds with T2 hyperintensity would be considered WMH on follow-up when evaluating FLAIR images only. In addition, we assessed imaging markers of SVD in a reliable and sensitive way, and calculated progression of WMH on the basis of all available time points utilizing a state-of-the-art deep learning–based segmentation algorithm. Finally, we carefully selected individuals with sporadic SVD, and excluded those with other or additional causes of acute ischemic stroke on the basis of data collected within the ongoing longitudinal RUN DMC study, and the additional carotid artery ultrasound and ECG made during the previsit of the current study.[14]

Some limitations should also be addressed. First, although we optimized our study protocol to detect DWI+ lesions, both in terms of spatial resolution of the DWI scan and frequency of scanning, we cannot rule out that we have missed (smaller) DWI+ lesions. However, although the general consensus is that the DWI signal is highest within the first 14 days after ictus, the signal evolution varies largely between individuals and may be elevated for at least 4 weeks.[8] Increasing the MRI frequency would have increased the likelihood of detecting more DWI+ lesions. However, we felt that this frequency would have seriously increased the attrition rate. Because only one small incident cavity could not be attributed to a DWI+ lesion on DWI 1 month prior to the event, we feel that this limitation has influenced our results only to a minor extent, although has potentially led to a slight underestimation of the contribution of DWI+ lesions to total SVD progression. Second, whereas recruitment of subjects from the 9-year follow-up RUN DMC study represents a major strength, this, together with the relatively small sample size (although the largest in its field), might limit the external validity of the observed incidence rate of DWI+ lesions within our study. In addition, despite applying stringent inclusion and exclusion criteria to rule out large artery disease and/or a cardioembolic source, we cannot completely rule out embolic sources as the possible cause of DWI+ lesions. Finally, although DWI+ lesions are highly suggestive of small acute ischemic strokes,[37] the acute ischemic nature of (clinically silent) DWI+ lesions in the context of SVD has not yet been confirmed. Diffusion restriction may also result from other conditions, including hypoglycemia, acute demyelination, or seizures, although these conditions are usually associated with a distinct topographical pattern on MRI and clinical presentation.[38,39] In addition, the cause of (micro)infarcts remains to be established, but an ischemic nature seems plausible, as previous studies suggest a role for hypoperfusion and microemboli.[9] Combined MRI–histopathology studies, and high-field quantitative imaging are required to shed new light on the nature and causes of DWI+ lesions.

In conclusion, DWI+ lesions are a marker of SVD, but their contribution to progression of SVD, in particular WMH, is minor. Our data imply that WMH progression is mostly driven by factors other than acute cerebral ischemia, awaiting future investigations.

Acknowledgment

A.M.T. was supported by the Dutch Heart Foundation (2016T044). B.G. and M.Du. were supported by the German Research Foundation (DU1626/1-1). C.J.M.K. and F.H.B.M.S. were supported by a clinical established investigator grant of the Dutch Heart Foundation (2012T077). C.J.M.K. was supported by an ASPASIA grant from the Netherlands Organization for Health Research and Development, ZonMw (015008048). F.-E.d.L. was supported by a clinical established investigator grant of the Dutch Heart Foundation (2014 T060), and by a VIDI innovational grant from the Netherlands Organization for Health Research and Development, ZonMw (016126351). M.Di. received funding from the Horizon 2020 research and innovation program of the European Union under grant agreement 666881, SVDs@target.

We thank M. I. Bergkamp for her assistance in the rating of the MRI scans; M. P. Noz for her assistance with collection of the data; and S. Ropele for his assistance in the calculation of the SWI scans.

Author Contributions

Study concept and design: A.t.T., A.M.T., M.Du., and F.-E.d.L.; data acquisition and analysis: all authors; drafting the manuscript or figures: A.t.T., K.W., B.G., A.M.T., M.Du., and F.-E.d.L.

Potential Conflicts of Interest

Nothing to report.

References

1. Debette S, Schilling S, Duperron M-G, et al. Clinical significance of magnetic resonance imaging markers of vascular brain injury: a systematic review and meta-analysis. JAMA Neurol 2018;76:81–94.
2. Wardlaw JM, Smith EE, Biessels GJ, et al. Neuroimaging standards for research into small vessel disease and its contribution to ageing and neurodegeneration. Lancet Neurol 2013;12:822–838.
3. Pantoni L. Cerebral small vessel disease: from pathogenesis and clinical characteristics to therapeutic challenges. Lancet Neurol 2010;9:689–701.
4. Joutel A, Chabriat H. Pathogenesis of white matter changes in cerebral small vessel diseases: beyond vessel-intrinsic mechanisms. Clin Sci (Lond) 2017;131:635–651.
5. Shi Y, Thrippleton MJ, Makin SD, et al. Cerebral blood flow in small vessel disease: a systematic review and meta-analysis. J Cereb Blood Flow Metab 2016;36:1653–1667.
6. Wardlaw JM, Smith C, Dichgans M. Mechanisms of sporadic cerebral small vessel disease: insights from neuroimaging. Lancet Neurol 2013;12:483–497.
7. Conklin J, Silver FL, Mikulis DJ, Mandell DM. Are acute infarcts the cause of leukoaraiosis? Brain mapping for 16 consecutive weeks. Ann Neurol 2014;76:899–904.
8. Schulz UG, Flossmann E, Francis JM, et al. Evolution of the diffusion-weighted signal and the apparent diffusion coefficient in the late phase after minor stroke: a follow-up study. J Neurol 2007;254:375–383.
9. van Veluw SJ, Shih AY, Smith EE, et al. Detection, risk factors, and functional consequences of cerebral microinfarcts. Lancet Neurol 2017;16:730–740.
10. Koch S, McClendon MS, Bhatia R. Imaging evolution of acute lacuner infarction: leukoariosis or lacune? Neurology 2011;77:1091–1095.
11. Pinter D, Gattringer T, Enzinger C, et al. Longitudinal MRI dynamics of recent small subcortical infarcts and possible predictors. J Cereb Blood Flow Metab 2018:0271678X18775215.
12. van Veluw SJ, Biessels GJ, Klijn CJ, Rozemuller AJ. Heterogeneous histopathology of cortical microbleeds in cerebral amyloid angiopathy. Neurology 2016;86:867–871.
13. van Veluw SJ, Lauer A, Charidimou A, et al. Evolution of DWI lesions in cerebral amyloid angiopathy: evidence for ischemia. Neurology 2017;89:2136–2142.
14. ter Telgte A, Wiegertjes K, Tuladhar AM, et al. Investigating the origin and evolution of cerebral small vessel disease: the RUN DMC - InTENse study. Eur Stroke J 2018;3:369–378.
15. van Norden AG, de Laat KF, Gons RA, et al. Causes and consequences of cerebral small vessel disease. The RUN DMC study: a prospective cohort study. Study rationale and protocol. BMC Neurol 2011;11:29.
16. Xu J, Moeller S, Auerbach EJ, et al. Evaluation of slice accelerations using multiband echo planar imaging at 3 T. Neuroimage 2013;83:991–1001.
17. Kellner E, Dhital B, Kiselev VG, Reisert M. Gibbs-ringing artifact removal based on local subvoxel-shifts. Magn Reson Med 2016;76:1574–1581.
18. Veraart J, Novikov DS, Christiaens D, et al. Denoising of diffusion MRI using random matrix theory. Neuroimage 2016;142:394–406.
19. Andersson JL, Sotiropoulos SN. An integrated approach to correction for off-resonance effects and subject movement in diffusion MR imaging. Neuroimage 2016;125:1063–1078.
20. Smith SM, Jenkinson M, Woolrich MW, et al. Advances in functional and structural MR image analysis and implementation as FSL. Neuroimage 2004;23:S208–S219.
21. Tustison NJ, Avants BB, Cook PA, et al. N4ITK: improved N3 bias correction. IEEE Trans Med Imaging 2010;29:1310–1320.
22. Soares JM, Marques P, Alves V, Sousa N. A hitchhiker's guide to diffusion tensor imaging. Front Neurosci 2013;7:31.
23. O'Brien KR, Kober T, Hagmann P, et al. Robust T1-weighted structural brain imaging and morphometry at 7T using MP2RAGE. PLoS One 2014;9:e99676.
24. Reuter M, Schmansky NJ, Rosas HD, Fischl B. Within-subject template estimation for unbiased longitudinal image analysis. Neuroimage 2012;61:1402–1418.
25. Duering M, Csanadi E, Gesierich B, et al. Incident lacunes preferentially localize to the edge of white matter hyperintensities: insights into the pathophysiology of cerebral small vessel disease. Brain 2013;136:2717–2726.
26. Li H, Jiang G, Zhang J, et al. Fully convolutional network ensembles for white matter hyperintensities segmentation in MR images. Neuroimage 2018;183:650–665.
27. Potter GM, Marlborough FJ, Wardlaw JM. Wide variation in definition, detection, and description of lacuner lesions on imaging. Stroke 2011;42:359–366.
28. Kuijf HJ, Brundel M, de Bresser J, et al. Semi-automated detection of cerebral microbleeds on 3.0 T MR images. PLoS One 2013;8:e66610.

29. Avants BB, Tustison NJ, Song G, et al. A reproducible evaluation of ANTs similarity metric performance in brain image registration. Neuroimage 2011;54:2033–2044.

30. Auriel E, Westover MB, Bianchi MT, et al. Estimating total cerebral microinfarct burden from diffusion-weighted imaging. Stroke 2015; 46:2129–2135.

31. Rosenberg GA. Extracellular matrix inflammation in vascular cognitive impairment and dementia. Clin Sci (Lond) 2017;131:425–437.

32. Havsteen I, Ovesen C, Willer L, et al. Small cortical grey matter lesions show no persistent infarction in transient ischaemic attack? A prospective cohort study. BMJ Open 2018;8:e018160.

33. Li F, Liu KF, Silva MD, et al. Transient and permanent resolution of ischemic lesions on diffusion-weighted imaging after brief periods of focal ischemia in rats: correlation with histopathology. Stroke 2000; 31:946–954.

34. ter Telgte A, van Leijsen EMC, Wiegertjes K, et al. Cerebral small vessel disease: from a focal to a global perspective. Nat Rev Neurol 2018;14:387–398.

35. Ferro DA, van den Brink H, Exalto LG, et al. Clinical relevance of acute cerebral microinfarcts in vascular cognitive impairment. Neurology 2019;92:e1558–e1566.

36. Lettau M, Laible M. 3-T high-b-value diffusion-weighted MR imaging in hyperacute ischemic stroke. J Neuroradiol 2013;40:149–157.

37. Gass A, Ay H, Szabo K, Koroshetz WJ. Diffusion-weighted MRI for the "small stuff": the details of acute cerebral ischaemia. Lancet Neurol 2004;3:39–45.

38. Sheerin F, Pretorius PM, Briley D, Meagher T. Differential diagnosis of restricted diffusion confined to the cerebral cortex. Clin Radiol 2008;63:1245–1253.

39. Karaarslan E, Arslan A. Diffusion weighted MR imaging in non-infarct lesions of the brain. Eur J Radiol 2008;65:402–416.